Caryologia
International Journal of Cytology, Cytosystematics and Cytogenetics

Firenze University Press
www.fupress.com/caryologia

OPEN ACCESS

Citation: V. Neves, W. Viegas, A. D. Caperta (2020) Effects of high temperature on mitotic index, microtubule and chromatin organization in rye (*Secale cereale* L.) root-tip cells. *Caryologia* 73(4): 55-63. doi: 10.13128/caryologia-788

Received: December 20, 2019

Accepted: July 27, 2020

Published: May 19, 2021

Data Availability Statement: All relevant data are within the paper and its Supporting Information files.

Competing Interests: The Author(s) declare(s) no conflict of interest.

Funding Statement: This work was funded by Portuguese national funds through Fundação para a Ciência e a Tecnologia (www.fct.pt/) project PTDC/AGRPRO/4285/2014, UI/AGR/04129/2013, and grant LEAF-AGR/04129/BPD/2015 to ADC.

Effects of high temperature on mitotic index, microtubule and chromatin organization in rye (*Secale cereale* L.) root-tip cells

Vânia Neves, Wanda Viegas, Ana D. Caperta*

Linking Landscape, Environment, Agriculture and Food (LEAF), Instituto Superior de Agronomia (ISA), Universidade de Lisboa, Tapada da Ajuda, 1349-017 Lisboa, Portugal
*Corresponding author. E-mail: anadelaunay@isa.ulisboa.pt

Abstract. Stressful high temperatures on plants can limit whole-plant function and decrease crop productivity. However, little is known regarding heat stress effects on microtubule cytoskeleton and chromatin in roots from intact plants. Here we studied high temperature effects on cell division, microtubule and chromatin organization patterns in rye root tips from intact plants subjected to 40°C for 4 h and after different recovery periods (0RT, 7RT, 24 RT). We showed that heat stress induced changes in nuclear morphology as detected by the unusual presence of interphase cells with irregularly shaped nuclei, probably associated with changes in chromosome segregation at anaphase, leading to micronuclei formation as well as changes in the mitotic index. These alterations were associated to differential effects in microtubules organization in both heat-stressed interphase and mitotic cells at 0RT and 7RT. Although no changes in the distribution of H3 phosphorylation of Ser 10 residues on chromatin were found in cells from heat-stressed plants, marked alterations in chromatin DNA methylation patterns were detected. These effects included higher agglutination of 5-methylcytosine domains in both interphase and metaphase cells compared to controls. Taken together these results seem to suggest that alterations in microtubule conformation upon heat stress influences nuclear chromatin organization and cell cycle progression. However, when seedlings recovered from stress (24RT), root tip cells presented microtubule configurations and chromatin organization patterns similar to controls. We conclude that in spite of heat stress markedly altered cell cycle progression and distribution of epigenetic marks, these responses are transient to cope with such stress conditions in the roots.

Keywords: DNA methylation, heat stress, histone H3 Ser 10 phosphorylation, microtubules, root.

INTRODUCTION

High temperature is one of major environmental factors limiting crop growth and yield worldwide causing many physiological changes that affect crop yield and quality (Suzuki et al. 2014). Most studies on these effects focus on the above-ground tissues such as shoot and reproductive organs,

although roots can also be subjected to high temperature stress which can limit whole plant function and decrease productivity (Heckathorn et al. 2013). A high degree of complexity in plant responses at the molecular, physiological and biochemical levels were described, largely controlled by different, and sometimes opposing, signaling pathways that may interact and inhibit each other (Suzuki et al. 2014). However, knowledge concerning combined microtubule (MT) cytoskeleton organization and chromatin nuclear topology upon heat stress in intact plants is scarce, particularly in roots.

In the plant cell cycle, the MT cytoskeleton composed of heteropolymers of α- and β-tubulin undergo dynamic conformational changes in a process known as dynamic instability in response to the needs of the cell (Horio and Murata 2014). Particularly, during cell division in somatic cells, MTs are arranged into characteristic structures like the interphase cortical MTs (CMT), pre-prophase band, mitotic spindle and phragmoplast (Baluska et al. 1998). Moreover, MTs can undergo a number of posttranslational modifications that act to control specific MTs-based functions in plants, including tyrosination, detyrosination, acetylation (Smertenko et al. 1997a), phosphorylation (Blume et al. 2008), polyglutamylation (Wang et al. 2004), and transamidation (Del Duca et al. 2009).

In plant cells disruption of MTs occurs in response to various environmental factors namely to extreme temperatures such as heat stress (*Nicotiana tabacum*, Smertenko et al. 1997a; Smertenko et al. 1997b; *Arabidopsis thaliana*, Müller et al. 2007), low temperature and abscisic acid treatments (*Triticum aestivum*, Khokhlova et al. 2003), hyperosmostic stress (*Triticum turgidum*, Komis et al. 2002), and affects post-translational modifications of tubulin as in cadmium stress (*Glycine max*, Gzyl et al. 2015). Furthermore, plant MTs in addition to their role in cell division and axial cell expansion, also have a thermosensory function that is of agronomical relevance in osmotic or cold stress conditions (*Triticum aestivum*, Abdrakhamanova et al. 2003; Nick 2012).

Moreover, plants response to drought, cold and high salinity stress involve several epigenetic regulatory mechanisms like both DNA and histone methylation and generation of small RNAs implicated in genome regulation and structure (Mirouze and Paszkowski 2011; Asensi-Fabado et al. 2017). Recent research has shown that environmental cues and abiotic stresses activate a stress memory that is mediated by epigenetic and chromatin-based mechanisms including chromatin modifications, such as cytosine methylation of DNA, histone methylation and nucleosome occupancy (Lämke and Bäurle 2017). For example, exposure of *Arabidopsis* plants to stresses, including salt, UVC, cold, heat and flood, resulted in a higher homologous recombination frequency, increased global genome methylation, and higher tolerance to stress in the untreated progeny. However, this transgenerational effect did not persist in successive generations (Boyko et al. 2010)..By contrast, prolonged heat stress induces transcriptional activation of several repetitive elements of *Arabidopsis thaliana* that requires minor changes in histone modifications but does not involve DNA demethylation (Pecinka et al. 2010). Patterns of DNA and histone modification can be altered in root tip cells of soybean seedlings grown at different temperatures (Stępiński 2012). During male meiosis in *Secale cereale* plants with B and without B chromosomes, heat exposure causes differential anomalies in chromatin structure in pachytene cells (Pereira et al. 2017). Heat-damaged pachytene cells displayed easily recognizable paired chromosome fibres and a single amorphous and heterochromatic mass closely associated with the nuclear periphery as well as disruption of the organization of sub-telomeric chromosome regions. However, no changes in DNA methylation patterns were detected in untreated and treated plants (Pereira et al. 2017).

In this work we investigated the effects of heat stress (40°C 4 h) on the organization of MT arrays and chromatin in rye root tips from intact seedlings, immediately after stress (0RT) and at different recovery periods (7RT, 24RT). In-depth cytological analyses of chromatin and microtubular organization were performed in root tip cells with DAPI, and immuno-labelling with antibodies against tubulin, 5-methylcytosine (5-mC) and histone H3 phosphorylated at serine 10 residue (H_3S_{10}ph).

MATERIALS AND METHODS

Plant material and heat stress conditions

Rye (*Secale cereale* L., $2n = 14$ chromosomes) seeds were kindly supplied by Neil Jones (Aberystwyth, UK). Seeds were placed in Petri dishes with moistened filter paper in the dark at 4°C for 3 days. Seedlings were transferred to a growth chamber with controlled light-temperature (Rumed), with a photoperiod of 18 h light and 6 h dark, at 25°C ± 2°C for 2 days. Then, seedlings were subdivided in two sets of experiments: (i) kept at 25°C ± 2°C with a photoperiod of 18 h light and 6 h dark (controls); and (ii) exposed to a ramp of increasing temperature from 25°C to 40°C (temperature increases 2°C / h), remaining 4 h at 40°C, after which the temperature fell gradually to 25°C (temperature decreases 2°C / h). The heat stress temperature was chosen based

on agronomical relevant temperatures shown to have a significant effect in cool season grasses such as rye (Xu, Zhan et al. 2011). All seedlings were kept moist during heat stress. Root tips were collected from plants in control conditions and from treated plants immediately after exposure to heat stress 40°C (0RT), and 7 h (7RT) and 24 h (24RT) during stress recovery.

Immunolabelling

For immunostaining of α-tubulin root tips were prepared as described in Caperta et al. (2006). Briefly, roots were fixed in freshly prepared 4% paraformaldehyde solution (PFA) containing MT stabilizing buffer (1xMTSB) for 45 min at room temperature, and then rinsed twice in 1xMTSB for 5 min. For H_3S_{10}ph immunodetection, root tips were fixed in freshly prepared 4% PFA solution containing phosphate-buffered saline (1xPBS, pH 7.3) for 30 min, and then washed three times for 5 min in 1x PBS according to Caperta et al. (2008). Immunostaining of 5-mC was performed in root tips fixed in ethanol:acetic acid (3:1) as described in Carvalho et al. (2010). For both H_3S_{10}ph and 5-mC immunolabelling, root tips were digested by treating with a pectolytic enzyme mixture [2% cellulase (Sigma), 2% cellulase "Onozuka R-10" (Serva), and 2% pectinase enzyme (Sigma) solution in 1xEB at 37º] until the material became soft.

The macerated material was squashed in 1xPBS or 1xMTSB on a slide. Slides were incubated for 1 h at 37ºC in a moisture chamber with a blocking solution (3% bovine serum albumin (BSA) in 1x PBS/1xMTSB, 0.1% Tween 20), followed by an incubation at 10ºC overnight with the primary antibody diluted in 1xPBS/MTSB supplemented with 1% BSA. After three washes in 1xPBS/MTSB for 5 min, the secondary antibodies diluted in 1xPBS/MTSB supplemented with 1% BSA were applied for 45 min at 37ºC. After final washes with 1xPBS, slides were counterstained with 4'6-diamino-2-phenylindole (DAPI) and mounted in 1mg/ml Citifluor antifade medium (AF1, Agar Scientific).

For MTs immunolocalization a mouse monoclonal antibody to α-tubulin (clone DM1A, Sigma, 1:100) was used, and the tyrosinated form of α-tubulin was detected with a rat antibody (YOL 1/2, Serotec, 1:100). An anti-mouse Alexa 488 antibody (Molecular Probes) and an anti-rat antibody conjugated with biotin (Serotec, 1:200) were used as secondary antibodies. This latter antibody was further detected with a streptavidin-Cy3 conjugate antibody (Sigma, 1:700). For detection of H_3S_{10}ph, a rabbit antibody (Upstate, 1:200) was utilized and revealed using anti-rabbit rhodamine-conjugated antibody (Dianova, 1: 100). For revealing 5-mC a primary mouse antibody (Abcam, 1:200) and a secondary antibody anti-mouse-Cy3 (Sigma, 1:100) were used. After three final washes, the slides were counterstained with DAPI and mounted in 1mg/ml Citifluor antifade medium (AF1, Agar Scientific). All samples were examined using a Zeiss Axioskop 2 epifluorescence microscope, images were obtained using a Zeiss AxioCam digital camera, and the digital images were processed with Photoshop (Adobe Systems).

Quantitative analysis of cell cycle progression and MT organization

The nuclear morphology of well-preserved cells from control and in distinct recovery periods (0, 7 and 24 RT) after treatment was determined and the percentage of DAPI stained cells with either regular or irregular shaped nuclei, and cells with micronuclei were calculated. Cell cycle was evaluated by calculating the mitotic index as the percentage of mitotic cells identified in at least n = 200 cells for each treatment. The number of mitotic cells at different phases was moreover evaluated through tubulin immunolocalization of particular MTs configurations (e.g. preprophase band, mitotic spindle or phragmoplast) in both control and heat-stressed cells after distinct periods of stress recovery. Effects of heat stress on CMTs organization were also evaluated in 200 cells from each treatment through the quantification of cells with normal or new MTs arrangements in distinct recovery periods. The Chi-square test (χ^2, $P< 0.05$) was utilized for statistical analysis.

RESULTS AND DISCUSSION

Changes in nuclear morphology and in mitotic index after heat stress are associated with new, transient MT arrangements

Interphase cells were classified as normal, when nuclei present regular shape and well-defined contour; abnormal, those showing nuclei with irregular shape; and cells with micronuclei. Most control cells (n = 200) showed normal interphase nuclei (94%, Table 1; Fig. 1a,b) and the mitotic index was 6%, but decreased immediately after heat stress (0RT – 3%, n=302). In 0RT cells a significant difference in nuclei types was detected in comparison with controls ($\chi^2 = 35.31$, $P< 0.05$), with an increase in the frequency of cells with abnormal nuclei (21%) and cells with micronuclei (3%). At 7RT cells (n = 300) significant differences between

Table 1. Percentage (%) of interphase cells with nuclear normal morphology (DAPI), tubulin immunolabeled cells in interphase (CMTs) and mitosis, and mitotic index. Control and heat-stressed cells analyzed after 0 (0 RT), 7 (7 RT), and 24 (24 RT) h of recovery from the stress. The presence of cortical microtubules (CMT), preprophase band (PPB), mitotic spindle (SP) and phragmoplast (P) was scored.

Seedlings treatments	Frequencies (%) of DAPI stained interphase cells with normal nuclear topology	Mitotic Index	Frequencies (%) of interphase cells with typical organized CMTs arrays	Frequencies of mitotic cells (%) at distinct phases			Number of mitotic cells analysed
				PPB	SP	P	
Control	94[a]	6[a]	98[a]	64[a]	24[a]	12	33
0 RT	76[b]	3[b]	16[b]	78[b]	11[b]	11	37
7 RT	53[c]	18[c]	37[c]	48[c]	27[a]	25	48
24 RT	90[a]	9[d]	95[a]	33[d]	48[c]	19	60

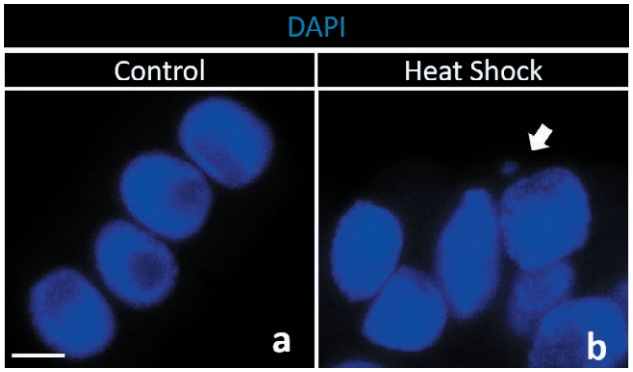

Figure 1. DAPI-stained *Secale cereale* meristematic interphase root cells. 1a – Control cells with a well-defined contour; and 1b. heat-stressed cells with irregular nuclei and/or with micronuclei (arrowed). Bar: 5 μm.

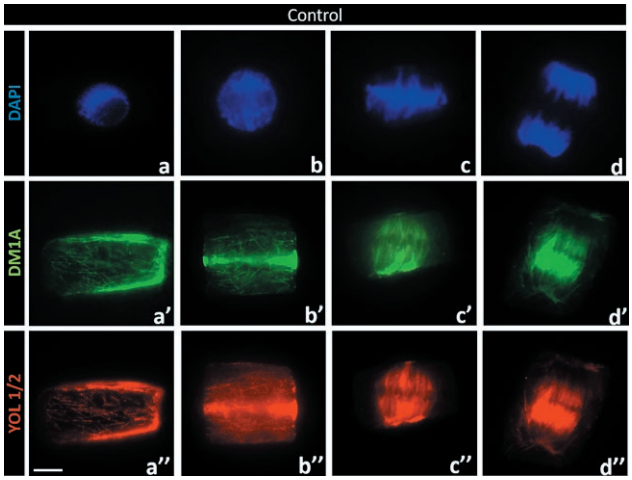

Figure 2. Indirect immunodetection of α-tubulin (MT) in control cells. Nuclei, chromatin and chromosomes are stained with DAPI (blue). Tubulin containing arrays are detected with DM1A α-tubulin (green) and YOL1/2 tyrosinated α-tubulin (red) antibodies. **a- a"** Interphase cell with cortical microtubules; **b- -b"** prophase cell with the preprophase band; **c -c"** meta/anaphase cell with spindle; **d- d"** ana/telophase cell with the phragmoplast. Bar: 5 μm.

heat-stressed cells and controls were found ($\chi^2 = 92.36$, $P< 0.05$) with a frequency of abnormal nuclei more than doubled (41%), and a small increase in cells with micronuclei (6%). The observed increase of micronuclei frequency attributable to root tips heat exposure is moreover associated with heat stress effects detected on mitotic cell cycle progression. The mitotic index was three times higher at 7RT (18%, Table 1) than in controls. Contrastingly, 24RT cells (n = 275) presented a high frequency of normal nuclei (90%) and a decrease in mitotic index (9%). The frequency of abnormal nuclei (7%) and micronuclei markedly decreased (3%). These findings support the hypothesis of mitotic arrest after 7RT of exposure to heat stress. Root tips exposure to diverse chemical substances including fertilizers, heavy metals, herbicides, pesticides and radioactivity also affect the mitotic index in varying frequencies in *Allium cepa* (Bonciu et al. 2018). Nonetheless, contrasting effects in the mitotic index were also observed in *Secale cereale* plants exposed to chemical stresses like the MTs-depolymerizing agent colchicine where mitotic arrest occurred in the low-concentration treatment, whereas c-metaphase cells were able to progress into the cell cycle in the high-concentration treatment (Caperta et al. 2006). Heat stress effects in nuclear morphology can also result from perturbations of CMTs organization as previously described for colchicine treatments (Caperta et al. 2006).

MTs configurations were analyzed in untreated and heat-treated root tips through tubulin immunolocalization using antibodies that recognize α-tubulin (DM1A) and tyrosinated tubulin (YOL 1/2). Our results show that both antibodies presented coincident and similar immuno-signal distributions (Fig. 2). Control cell MTs exhibited both α-tubulin and tyrosinated tubulin arrays

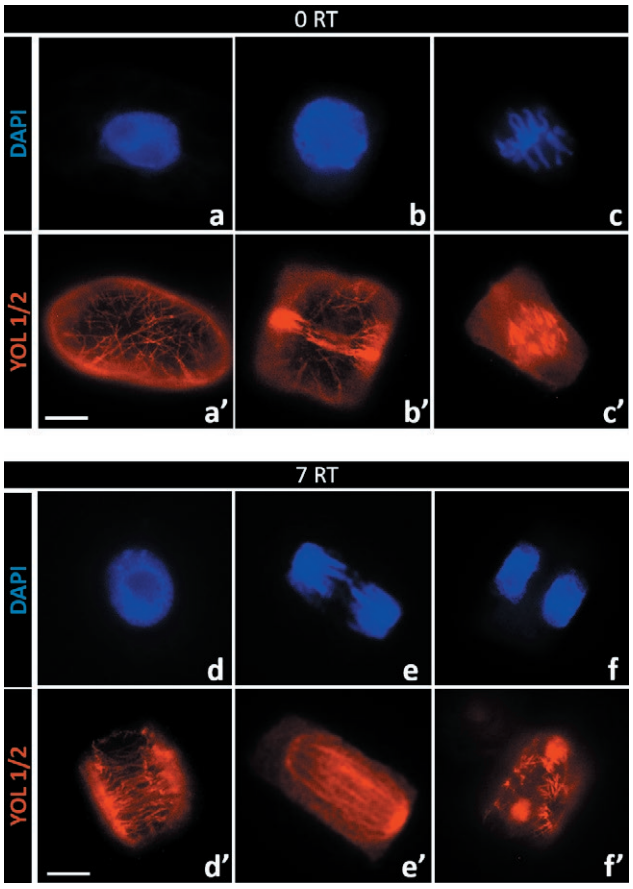

Figure 3. Indirect immunodetection of α-tubulin (MT) in heat-stressed cells after 0 (0 RT), 7 (7 RT), and 24 (24 RT) h of recovery from the stress. Nuclei, chromatin and chromosomes are stained with DAPI (blue). Tubulin containing arrays are detected with YOL1/2 tyrosinated α-tubulin (red) antibody. **a-a'** and **d-d'** Interphase cells showing branched, stringy CMTs with disorganized orientation; **b-b'** prophase cell with a slightly disorganized pre-prophase band with MTs without the usual parallel orientation; metaphase cell (**c-c'**) and anaphase cell (**e-e'**) with normal spindles; **f-f'** telophase cell with thick CMTs arrays and with remnants of phragmoplast. Bar: 5 μm.

configurations characteristic of higher plant cells: CMTs at interphase, pre-prophase band, mitotic spindle and phragmoplast at the end of telophase (Fig. 1). Control cells presented organized CMTs (98%, Table 1), whereas at 0RT significant differences occurred (χ^2 = 687. 57, P< 0.05), in which the majority of cells exhibited branched and wavy CMTs with a disorganized orientation (84%) (Fig. 3a-a'). Previous studies showed that heat stress caused dissemblance of MTs in mitotic tobacco suspension cultured cells after 30 min at 42°C (Smertenko et al. 1997b). In the present study we showed higher resilience of rye MTs to heat stress since exposure of 2 days seedlings to 4 h at 40°C only induced CMTs disorganization at 0RT without total disruption. However, knowledge is inexistent with regard to the heat response of the rye variety used in this study (heat-resistant or heat-sensitive). Compared to controls, at 7RT there was still a significant difference in the frequency of interphase cells with a disorganized and branched wavy-like MTs configuration (63%, Table 1, Fig. 3d-d') (χ^2 = 424. 97, P< 0.05), although the frequency of interphase cells with normal MTs arrangements doubled. At 24RT 95% of interphase cells present typical organized CMT arrays (Table 1). Disorganized wavy MTs arrangements were also observed in root cells exposed to high colchicine concentration conditions (Lazareva et al. 2003; Caperta et al. 2006). Therefore, it is tempting to suggest that new MTs re-orientations result from perturbations induced by heat stress on CMTs associations with plasma membrane, although the nature of MT attachments to the membrane is not yet totally clear both in animal (Wolff 2009) and in plant cells despite all efforts to understand it (Liu et al. 2015). It was demonstrated that CMTs can change their orientation in response to a broad range of abiotic signals (Nick 2013) by controlling the direction of cellulose deposition and reinforcing axial cell expansion (Geitmann and Ortega 2009). In the current work, the high frequency of interphase cells with abnormal nuclear morphology observed at 7RT probably reflects changes in CMTs organization by inducing differential cytosol compartmentalization.

Earlier studies moreover reported that different MTs arrays presented distinct sensitivities to temperature stress (Smertenko et al. 1997b; Abdrakhamanova et al. 2003; Müller et al. 2007). The most heat-sensitive MT arrays are those of the mitotic spindle and the phragmoplast in tobacco cultured cells (Smertenko et al. 1997b). In *Triticum* chilling sensitive species, CMTs are extremely cold-sensitive, whereas they persist at low temperatures in chilling-tolerant species (Abdrakhamanova et al. 2003). In this study, MTs from the pre-prophase band (PPB) appeared to be very sensitive to heat stress since most prophase cells at 0RT (94%) presented slightly disorganized pre-prophase bands (Fig. 3b-b'). Such marked changes in frequencies of prophase cells with abnormal PPB at 0RT were however not associated with perturbations in other mitotic phases since all metaphase (Fig. 3c-3c') and anaphase cells exhibited well-formed spindles, and telophase cells showed phragmoplast MTs orthogonally disposed to the division plane. After 7RT, most prophase cells presented a reduction of abnormal pre-prophase bands (65%), although in some cells altered spindle and phragmoplast configurations were revealed (Fig. 3f-f'), which were absent at 24RT.

Compared to controls, the frequency of cells with PPBs presented the highest value at 0RT (78%) and the

lowest one at 24RT (33%). These findings contrasted with frequencies of cells with spindles and phragmoplasts, which have low frequencies at 0RT (22%) and high frequencies at 7RT (52%), with a maximum of at 24RT (67%). Taken together, the drastic dropping of mitotic index values at 0RT seems to be associated with perturbations on CMTs organization as well as disturbances on PPB allowing however the progression of subsequent mitotic phases as only cells with normal spindles and phragmoplasts were detected. On the other hand, at 7RT the observed beginning of normal CMT organization reestablishment seemed to allow cells transition to mitosis associated with the marked increase in the mitotic index. The high frequencies of cells in metaphase, anaphase and cytokinesis at 7RT, associated with some perturbations in spindle and phragmoplast organizations appear to indicate why heat-stressed cells stay longer in mitosis. After 24 RT the MT cytoskeleton configurations in interphase and prophase cells were like the ones observed in controls, although the high frequencies of cells at metaphase, anaphase and cytokinesis revealed a delayed reestablishment reflected in the high mitotic index yet observed. Nonetheless, it is not yet clear which microtubule structures, cortical MTs or mitotic MTs, are susceptible to tubulin modification induced by heat stress.

Heat stress induces changes in DNA methylation patterns but no alterations in $H_3S_{10}ph$ distribution patterns

In both control and heat-stressed cells $H_3S_{10}ph$ marks were absent during interphase. However, they were present in prophase cells in the pericentromeric heterochromatin and restricted to one nuclear hemisphere revealing Rabl configuration (Fig. 4). The Rabl configuration, characteristic of rye genome (Caperta et al. 2002) is maintained after heat stress as centromeres are all aligned in one nuclear pole. In interphase cells no labelling was found (Fig. 4a-a'), which contrasted with prophase (Fig. 4b-b'), metaphase (Fig. 4a-a' and c-c') and anaphase (Fig. 4a-a') cells. In mitotic cells, a marked labelling was also found in chromosomes pericentromeric regions but no detectable changes were observed in signal dimensions or intensities in both control and heat-stressed cells (Figs. 4d-d', 4e-e', 4f-f'). Instead, cold treatment of plant root meristems resulted in additional chromosomal sites of $H_3S_{10}ph$, besides the usual ones in pericentromeric regions (Manzanero et al. 2000). Also, up-regulation of the stress-inducible genes in *Arabidopsis* T87 and tobacco BY-2 cell lines is associated with increased phosphorylation of histone H3 at serine 10 residue at high salinity, cold and abscisic acid treatments (Sokol et al. 2007).

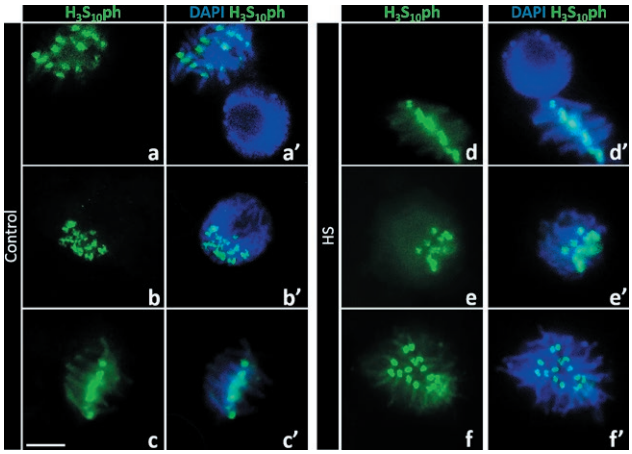

Figure 4. Indirect immunodetection of histone H3 phosphorylated at serine 10 residue in *Secale cereale* meristematic root cells. Nuclei, chromatin and chromosomes are stained with DAPI (blue). Chromatin and chromosomes are detected with histone H3 phosphorylated at serine 10 residue ($H_3S_{10}ph$, green) antibody in control (a-a'- c-c') and heat-stressed cells (d-d'- f-f'). **a-a'** Interphase cell without $H_3S_{10}ph$ labelling and an anaphase cell with $H_3S_{10}ph$ marks; **b-b'** prophase cells showing $H_3S_{10}ph$ marks in the pericentromeric heterochromatin and restricted to one nuclear hemisphere revealing Rabl configuration; **c-c'** metaphase cell presenting $H_3S_{10}ph$ dots only in a discrete region in pericentromeric chromatin; **d-d'** cell at interphase showing no $H_3S_{10}ph$ labelling and a metaphase cell with pericentromeric $H_3S_{10}ph$ immnosignals; **e-e'** cell at prophase with $H_3S_{10}ph$ marks in the pericentromeric heterochromatin; and **f-f'** early anaphase cell revealing $H_3S_{10}ph$ dots only in pericentromeric chromatin. Bar: 5 μm.

Control cells showed interphase nuclei with disperse, dotted and intense 5-mC immunosignal all over the nucleus both in highly condensed (heterochromatin) and decondensed (euchromatin) chromatin (Fig. 5a-a''). Instead, in heat-stressed cells at 0RT and 7RT a distinct, heterogeneous DNA methylation distribution pattern with aggregated immunosignal was preferentially found more concentrated in the nuclear periphery (Fig. 5c-c'' and 5d-d''). In metaphase cells, at both 0RT and 7RT a heterogeneous and discontinuous 5-mC labeling was also detected along chromosome arms (Fig. 5e-e''). After 24 RT, the distribution patterns of 5-mC were like those observed in control interphase and metaphase cells (Fig. 5f-f'''). The results presented here in rye somatic cells from control plants are in accordance with earlier studies in rye metaphase chromosome spreads, which displayed a punctuated and uniform pattern of methylated DNA residues along both the As and Bs chromosomes, without any particular sites of accumulation (Carchilan et al. 2007). However, no differences were found in the nuclear distribution of methylated cytosines between meiocytes of heat-stressed and control rye plants with

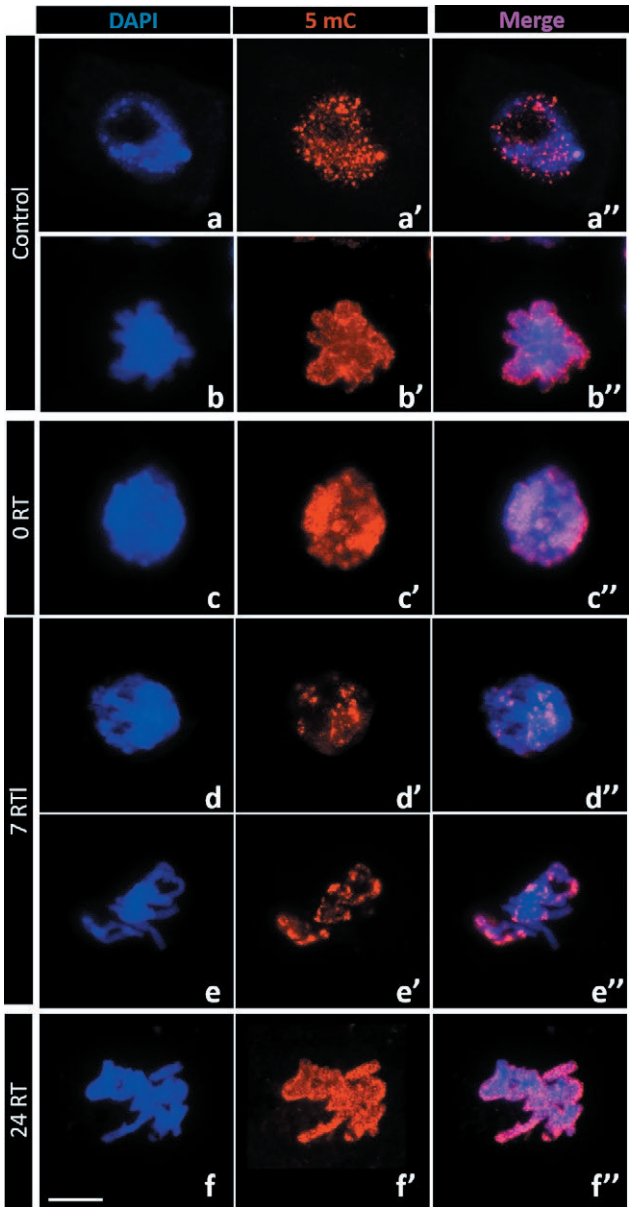

Figure 5. Indirect immunodetection of 5-methylcytosine in *Secale cereale* meristematic root cells. Control and heat-stressed cells were analysed after 0 (0 RT), 7 (7 RT), and 24 (24 RT) h of recovery from the stress. Nuclei, chromatin and chromosomes are stained with DAPI (blue). Chromatin and chromosomes are detected with 5-methylcytosine (5-mC, red) antibody. **a-a"** Control interphase and **b-b"** metaphase cells with homogenous 5-mC labelling; **c-c"** and **d-d"** heat-stressed interphase nuclei with a heterogeneous distribution pattern of 5-mC exhibiting aggregated immunosignals in the nuclear periphery; **e-e"** an heterogeneous discontinuous 5-mC labelling along chromosome arms of a metaphase cell; **f-f'"**metaphase cell showing a homogenous 5-mC labelling after 24RT. Bar: 5 μm.

0B or 2B chromosomes (Pereira et al. 2017). A study on the effects of heat stress in the repetitive sequence genome fraction (coding and non-coding sequences) using leaves of intact rye plants suggests marked differences between these sequences that most likely reflect their distinct roles in the plant pathways involved in the stress response (Tomás et al. 2013).

Hence, it appears that there are different temperature chromatin sensitivities accordingly with chromatin fractions, cell types and tissue origins. For instance, in soybean at normal temperature, root hairs were more hypermethylated than were stripped roots whereas in response to heat stress, both root hairs and stripped roots showed hypomethylation (Hossain et al. 2017). These changes in DNA methylation were directly or indirectly associated with expression of genes and transposons within the context of either specific tissues/cells or heat stress (Hossain et al. 2017). Other studies in which both roots and above-ground tissues were heat-stressed indicate that roots are often more sensitive to heat stress than shoots in terms of cell division and physiological responses (Heckathorn al. 2013). We conclude that heat stress induces transient changes in chromatin and MT organization rye root seedlings, which might indicate cell adjustments in stressful conditions.

ACKNOWLEDGEMENTS

Thanks to Augusta Barão (ISA) for excellent technical assistance, and two anonymous reviewers for valuable comments on the manuscript, which improved its quality.

REFERENCES

Abdrakhamanova A, Wang QY, Khokhlova L, Nick P. 2003. Is microtubule assembly a trigger for cold acclimation? Plant Cell Physiol. 44:676-686.

Asensi-Fabado MA, Amtmann A, Perrella, G. 2017. Plant responses to abiotic stress: the chromatin context of transcriptional regulation. BBA 1860(1):106-122.

Baluska F, Volkmann D, Barlow PW. 1998. Tissue- and development-specific distributions of cytoskeletal elements in growing cells of the maize root apex. Plant Biosyst. 132:251-65.

Blume YB, Yemets A, Sulimenko V, Sulimenko T, Chan J, Lloyd C, Dráber P. 2008. Evidence of tyrosine phosphorylation of plant tubulin. Planta 229:143-150.

Bonciu E, Firbas P, Fontanetti CS, Wusheng J, Karaismailoğlu MC, Liu D, Menicucci F, Pesnya DS, Popescu A, Romanovsky AV, Schiff S, Ślusarczyk J, de Souza CP, Srivastava A, Sutan A, Papini A. 2018. An evaluation for the standardization of the *Allium cepa*

test as cytotoxicity and genotoxicity assay. Caryologia 71(3):191-209.

Boyko A, Blevins T, Yao Y, Golubov A, Bilichak A, llnytskyy Y, Hollander J, Meins F, Kovalchuk I. 2010. Transgenerational adaptation of *Arabidopsis* to stress requires DNA methylation and the function of dicer-like proteins. PLoS ONE 5(3):e9514.

Caperta AD, Neves N, Morais-Cecílio L, Malhó R, Viegas W. 2002. Genome restructuring in rye affects the expression, organization and disposition of homologous rDNA loci. J Cell Sci. 115(14):2839-2846.

Caperta A, Delgado M, Ressurreição F, Meister A, Jones R, Viegas W, Houben A. 2006. Colchicine-induced polyploidization depends on tubulin polymerization in c-mitotic cells. Protoplasma 227:147-153.

Caperta A, Rosa M, Delgado M, Karimi D, Demidov D, Viegas W, Houben A. 2008. Distribution patterns of phosphorylated Thr 3 and Thr 32 of histone H3 in mitosis and meiosis of plants. Cytogenet Genome Res. 122:73-79.

Carvalho A, Delgado M, Barão A, Frescatada M, Ribeiro E, Pikaard CS, Viegas W, Neves N. 2010. Chromosome and DNA methylation dynamics during meiosis in the autotetraploid *Arabidopsis arenosa*. Sex Plant Reprod. 23:29–37.

Carchilan M, Delgado M, Ribeiro T, Costa-Nunes P, Caperta A, Morais-Cecílio L, Jones RN, Viegas W, Houben A. 2007. Transcriptionally active heterochromatin in rye B chromosomes. Plant Cell 19:1738–1749.

Del Duca S, Serafini-Fracassini D, Bonner PL, Cresti M, Cai G. 2009. Effects of post-translational modifications catalysed by pollen transglutaminase on the functional properties of microtubules and actin filaments. Biochem J. 418:651-664.

Geitmann A, Ortega JK. 2009. Mechanics and modeling of plant cell growth. Trends Plant Sci. 14(9):467-478.

Gzyl J, Chmielowska-Bąk J, Przymusiński R, Gwóźdź EA. 2015. Cadmium affects microtubule organization and post-translational modifications of tubulin in seedlings of soybean (*Glycine max* L.). Front Plant Sci. 6:937.

Heckathorn SA, Giri A, Mishra S, Bista D. 2013. Heat stress and roots. In: Tuteja N, Gill SS, editors. Climate change and plant abiotic stress tolerance. Germany: Wiley-VCH Verlag GmbH & Co. KGaA, p. 109-136.

Horio T, Murata T. 2014. The role of dynamic instability in microtubule organization. Front. Plant Sci. 5:511.

Hossain MS, Kawakatsu T, Kim KD, Zhang N., Nguyen CT, Khan SM, Batek JM, Joshi T, Schmutz J, Grimwood J, Schmitz RJ, Xu D, Jackson SA, Ecker JR, Stacey G. 2017. Divergent cytosine DNA methylation patterns in single-cell, soybean root hairs. New Phytol. 214(2):808-819.

Khokhlova LP, Olinevich OV, Raudaskoski M. 2003. Reorganization of the microtubule and actin cytoskeleton in root cells of *Triticum aestivum* L. during low temperature and abscisic acid treatments. Cell Biol Int. 27(3):211-212.

Komis G, Apostolakos P, Galatis B. 2002. Hyperosmotic stress induced formation of tubulin macrotubules in root-tip cells of *Triticum turgidum*: their probable involvement in protoplast volume control. Plant Cell Physiol. 43:911–922.

Lämke J, Bäurle I. 2017. Epigenetic and chromatin-based mechanisms in environmental stress adaptation and stress memory in plants. Gen Biol 18(1):124.

Lazareva EM, Polyakov VY, Chentsov YS, Smirnova EA. 2003. Time and cell cycle dependent formation of heterogeneous tubulin arrays induced by colchicine in *Triticum aestivum* root meristem. Cell Biol Int. 27:633–646.

Liu Z, Persson S, Zhang Y. 2015. The connection of cytoskeletal network with plasma membrane and the cell wall. Journal of Integrative Plant Biol. 57(4):330-340.

Manzanero S, Arana P, Puertas MJ, Houben A. 2000. The chromosomal distribution of phosphorylated histone H3 differs between plants and animals at meiosis. Chromosoma 109(5):308-317.

Mirouze M, Paszkowski J. 2011. Epigenetic contribution to stress adaptation in plants. Curr Opin Plant Biol. 14(3):267-274.

Müller J, Menzel D, Šamaj J. 2007. Cell-type-specific disruption and recovery of the cytoskeleton in *Arabidopsis thaliana* epidermal root cells upon heat shock stress. Protoplasma 230:231–242.

Nick P. 2012. Microtubules and the tax payer. Protoplasma 249(2):81-94.

Nick P. 2013. Microtubules, signalling and abiotic stress. Plant J. 75(2:309-323.

Pecinka A, Dinh HQ, Baubec T, Rosa M, Lettner N, Scheid OM. 2010. Epigenetic regulation of repetitive elements is attenuated by prolonged heat stress in *Arabidopsis*. Plant Cell 22(9):3118-3129.

Pereira HS, Delgado M, Viegas W, Rato JM, Barão A, Caperta AD. 2017. Rye (*Secale cereale*) supernumerary (B) chromosomes associated with heat tolerance during early stages of male sporogenesis. Ann Bot. 119:325–337.

Smertenko A, Blume Y, Viklický V, Opatrný Z, Dráber P. 1997a. Posttranslational modifications and multiple tubulin isoforms in *Nicotiana tabacum* cells. Planta 201:349-358.

Smertenko A, Dráber P, Viklický V, Opatrný Z. 1997b. Heat stress affects the organization of microtubules and cell division in *Nicotiana tabacum* cells. Plant Cell Environ. 20:1534-1542.

Sokol A, Kwiatkowska A, Jerzmanowski A, Prymakowska-Bosak M. 2007. Up-regulation of stress-inducible genes in tobacco and *Arabidopsis* cells in response to abiotic stresses and ABA treatment correlates with dynamic changes in histone H3 and H4 modifications. Planta 227:245–254.

Suzuki N, Rivero RM, Shulaev V, Blumwald E, Mittler R. 2014. Abiotic and biotic stress combinations. New Phytol. 203(1):32-43.

Stępiński D. 2012. Levels of DNA methylation and histone methylation and acetylation change in root tip cells of soybean seedlings grown at different temperatures. Plant Physiol Bioch. 61: 9-17.

Tomás D, Brazão J, Viegas W, Silva M. 2013. Differential effects of high-temperature stress on nuclear topology and transcription of repetitive noncoding and coding rye sequences. Cytogenet Genome Res. 139(2):119-127.

Wang W, Vignani R, Scali M, Sensi E, Cresti M. 2004. Post-translational modifications of α-tubulin in *Zea mays* L. are highly specific. Planta 218(3):460-465.

Wolff J. 2009. Plasma membrane tubulin. Biochim Biophys Acta - Biomembranes 1788(7):1415-1433.

Xu Y, Zhan C, Huang B. 2011. Heat shock proteins in association with heat tolerance in grasses. Int J Proteomics. 2011:2011.